

Received 27 October 2022

Accepted 1 November 2022

Edited by W. T. A. Harrison, University of Aberdeen, United Kingdom

Keywords: crystal structure; biipyridine ligand; photophysical properties; DFT calculation.**CCDC reference:** 2216704**Supporting information:** this article has supporting information at journals.iucr.org/e

Synthesis, crystal structure and DFT calculations of (2',6'-difluoro-2,3'-bipyridine- κN^2)[2,6-difluoro-3-(pyridin-2-yl)phenyl- $\kappa^2 C^1, N^3$]methylplatinum(II)

Suk-Hee Moon,^a Seohyeon Choi^b and Youngjin Kang^{b*}

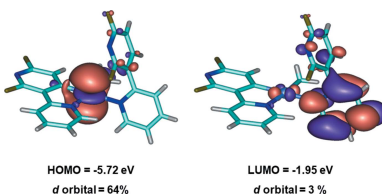
^aDepartment of Food and Nutrition, Kyungnam College of Information and Technology, Busan 47011, Republic of Korea, and ^bDivision of Science Education, Kangwon National University, Chuncheon 24341, Republic of Korea.

*Correspondence e-mail: kangy@kangwon.ac.kr

The title compound, $[\text{Pt}(\text{CH}_3)(\text{C}_{10}\text{H}_5\text{F}_2\text{N}_2)(\text{C}_{10}\text{H}_6\text{F}_2\text{N}_2)]$, displays a distorted *cis*- PtN_2C_2 square-planar geometry around the Pt^{II} ion consisting of the bidentate C, N chelating anion, a monodentate N -bonded neutral ligand and a methyl group. In the crystal, the molecules are linked by $\text{C}-\text{H}\cdots\text{F}$, $\text{C}-\text{H}\cdots\text{N}$ and $\text{C}-\text{H}\cdots\pi$ interactions. Time-dependent density functional theory (TD-DFT) at the B3LYP level with the 6-311++G(d,p) basis set was applied to optimize the ground-state geometry. The electronic properties, such as excitation energies and the HOMO–LUMO gap energies, were calculated and compared to related structures.

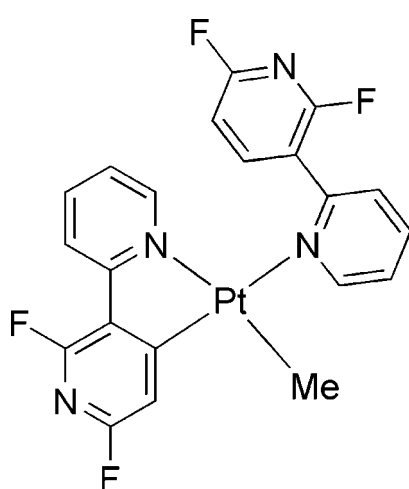
1. Chemical context

Over the past two decades, there has been considerable interest in the design of phosphorescent Ir^{III} and Pt^{II} complexes based on C, N -chelating ligands, especially 2',6'-difluoro-2,3'-bipyridine (dfpypy) (Kang *et al.*, 2022*b,c*; Zaen *et al.*, 2019). Among them, heteroleptic Pt^{II} compounds show high thermal stability and photoluminescence quantum efficiency (PLQY). Both characteristics make them suitable for applications as organic light-emitting diodes (OLEDs) and organic lighting (Kang *et al.*, 2021; Lee *et al.*, 2018). Despite the many advantages of Pt^{II} complexes based on bipyridine ligands, there are some problems that need to be addressed. For example, a gradient efficiency roll-off often occurs at high current densities owing to intrinsic triplet-triplet exciton annihilation (Zhang *et al.*, 2020). To overcome this limitation, it is necessary to develop heavy transition-metal compounds with octahedral geometry. Therefore, Pt^{IV} complexes are highly desirable in OLED applications compared with those of their Pt^{II} analogues. However, reports on Pt^{IV} compounds based on C, N chelates are scarce, despite the compounds having similar geometries and electronic configurations to Ir^{III} complexes. To make C, N -based Pt^{IV} octahedral complexes, the syntheses of Pt^{II} complexes are needed as intermediates at the first step (Juliá *et al.*, 2016). However, the structures and photophysical properties of these Pt^{II} precursors are still scarce, which prompted us to determine the structure of a Pt^{II} complex bearing a C, N chelating dfpypy ligand and investigate its photophysical properties (Juliá & González-Herrero, 2016). Herein, we describe the results of our investigation regarding the structural characterization, photophysical properties, and TD-DFT calculations of the title dfpypy-based Pt^{II} compound.



OPEN ACCESS

Published under a CC BY 4.0 licence



2. Structural commentary

The molecular structure of the title compound is shown in Fig. 1. Of the two 2,3'-bipyridyl units, the N1-containing pyridine ring is slightly tilted by $3.08(7)^\circ$ to the N2-containing one, while the N3-containing pyridine ring is almost perpendicular to N4-containing one with a dihedral angle of $80.95(9)^\circ$. As expected, the title compound has a distorted PtN_2C_2 square-planar geometry around the platinum center with an *N,N-cis* structure (Table 1). The Pt–C and Pt–N bond lengths for the title compound are within the range reported for those of related compounds, namely $[\text{Pt}(\text{dfppy})_2(\text{Me})\text{Cl}]$ and $[\text{Pt}(\text{ppy})_2(\text{Me})\text{Cl}]$ (ppy = 2-phenylpyridine) (Kang *et al.*, 2022a; Juliá *et al.*, 2016). The Pt1–N1 bond length in the title compound [$2.0943(3)$ Å] is similar to that of Pt1–

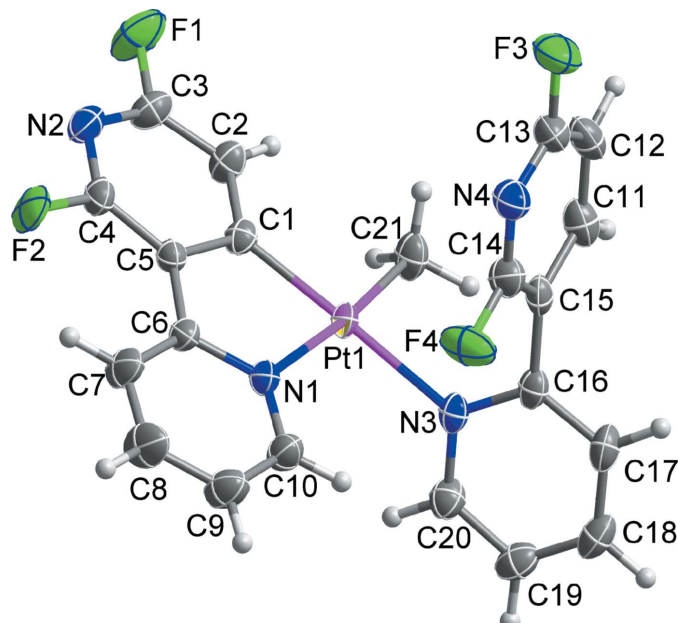


Figure 1

The molecular structure of the title compound, with the atom-numbering scheme. Displacement ellipsoids are drawn at the 30% probability level.

Table 1
Selected geometric parameters (\AA , $^\circ$).

Pt1–C1	1.966 (3)	Pt1–N1	2.094 (3)
Pt1–C21	2.036 (4)	Pt1–N3	2.120 (3)
C1–Pt1–C21	92.94 (14)	C1–Pt1–N3	177.73 (12)
C1–Pt1–N1	81.10 (12)	C21–Pt1–N3	89.33 (13)
C21–Pt1–N1	174.00 (12)	N1–Pt1–N3	96.63 (10)

N3 [$2.120(3)$ Å]. However, the Pt1–C21 bond length [$2.036(4)$ Å] is significantly longer than that of Pt1–C1 [$1.966(3)$ Å]; this is attributed to the greater *trans* influence exerted by the N atom of the C,N ligand located at the *trans* position and the lack of π -back bonding between the Pt atom and the C atom of the methyl ligand.

3. Supramolecular features

In the extended structure, C–H \cdots F/N hydrogen bonds (Table 2, yellow dashed lines in Fig. 2) between adjacent molecules lead to the formation of a di-periodic supramolecular network. The network is consolidated by weak aromatic π – π stacking, C–H \cdots π and C–F \cdots π interactions [red, sky-blue, and black dashed lines in Fig. 2, respectively; $Cg2\cdots Cg3^i = 3.865(2)$ Å; $C21\cdots H21A\cdots Cg4^{ii} = 3.507(4)$ Å; $C3\cdots F1\cdots Cg1^{iii} = 3.968(3)$ Å; $C13\cdots F3\cdots Cg3^{iv} = 3.472(3)$ Å; $Cg1$, $Cg2$, $Cg3$ and $Cg4$ are the centroids of the N1/C6–C10,

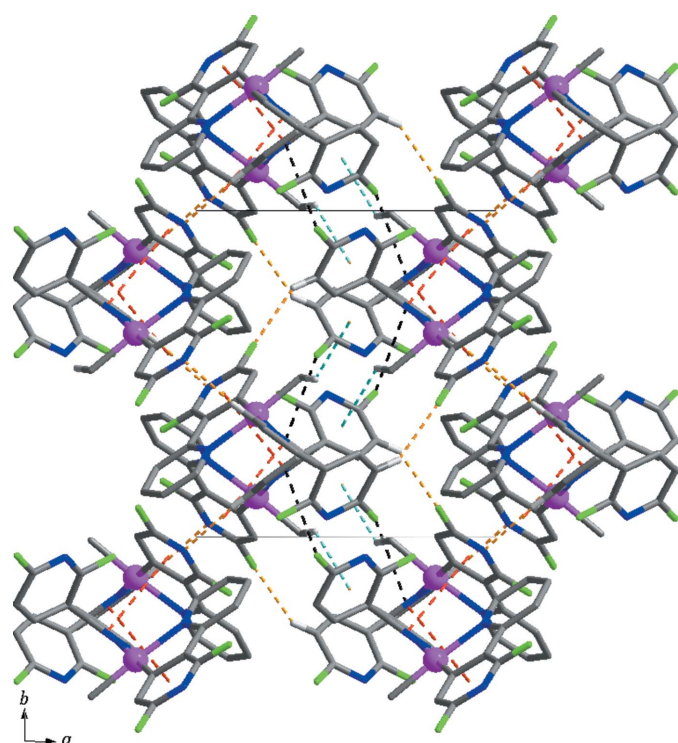


Figure 2

The di-periodic supramolecular network formed through C–H \cdots F/N hydrogen bonds (yellow dashed lines), F \cdots π (black dashed lines) C–H \cdots π (sky-blue dashed line) and π – π (red dashed lines) stacking interactions. For clarity, H atoms not involved in the intermolecular interactions have been omitted.

Table 2
Hydrogen-bond geometry (\AA , $^\circ$).

$D-\text{H}\cdots A$	$D-\text{H}$	$\text{H}\cdots A$	$D\cdots A$	$D-\text{H}\cdots A$
C7—H7···F2	0.95	2.24	2.858 (4)	122
C12—H12···F1 ⁱ	0.95	2.44	3.259 (5)	144
C20—H20···N2 ⁱⁱ	0.95	2.45	3.385 (5)	167

Symmetry codes: (i) $-x + 1, -y + 1, -z + 1$; (ii) $-x + 2, -y + 1, -z + 1$.

N2/C1—C5, N3/C16—C20 and N4/C11—C15 rings, respectively; symmetry codes: (i) $x, -y + \frac{3}{2}, z + \frac{1}{2}$; (ii) $-x + 1, y - \frac{1}{2}, -z + \frac{1}{2}$; (iii) $-x + 2, -y + 1, -z + 1$; (iv) $-x + 1, y + \frac{1}{2}, -z + \frac{1}{2}$. These varied interactions presumably assist in the stabilization of the network structure.

4. Photophysical properties

The absorption and emission spectra of title compound in solution are shown in Fig. 3. The title compound exhibits a similar absorption pattern in the 230–350 nm range, as compared to its analog [Pt(ppy)(ppyH)(Me)] (Juliá & González-Herrero, 2016). The most intense absorption band at 235 nm is assigned to a $\pi-\pi^*$ ligand-centered (^1LC) transition, and the next weak absorption band at longer wavelengths (380–440 nm) is assigned to a metal-to-ligand charge-transfer (MLCT) transition. The title compound shows weak blue and non-structured emission in CH_2Cl_2 solution at ambient temperature at approximately 455 nm, which is much shorter than that of the parent molecule, [Pt(ppy)(ppyH)(Me)] ($\lambda_{\text{max}} = 468$). Therefore, the blue-shifted absorption and emission could be due to the greater triplet energy of dfppy relative to that of ppy.

5. TD-DFT calculations

To gain deeper insight into the geometrical configuration and nature of the luminescence properties, we performed TD-DFT calculations in the gas phase. Molecular orbital calculations were performed using the Gaussian 03 (Frisch *et al.*,

2004) program. Fig. 4 shows the HOMO and LUMO energy levels of the optimized structures obtained from the single-crystal structure. The TDDFT results show that the triplet vertical excitation at the ground-state geometry corresponds to a $\pi(\text{dfppy})/\text{d}(\text{Pt}) \rightarrow \pi^*(\text{dfppy})$ electronic promotion ($^3\text{LC}/\text{MLCT}$). The HOMO level has significant contributions from the d orbital (64%) of Pt^{II} , with small contributions from the C-coordinating dfppy. Notably, there is little contribution from N-coordinating dfppy at the HOMO level. By contrast, the contribution from the π^* orbitals of the dfppy chelate is very significant at the LUMO level, whereas the contribution from the Pt^{II} atom is negligible. Thus, the electronic transition might arise from ligand-centered charge transfer [LCCT, $\pi(\text{dfppy})-\pi^*(\text{dfppy})$] mixed with metal-to-ligand charge transfer [MLCT, $(\text{Pt}(d)-\pi^*(\text{dfppy}))$]. The HOMO energy level is -5.72 eV, which is much lower than that of its analogues, such as [Pt(ppy)(ppyH)(Me)] ($E_{\text{HOMO}} = -5.27$ eV). This lower HOMO energy level may be attributed to the replacement of the fluorine-substituted pyridine at the C,N chelate. The calculated LUMO energy is -1.95 eV and the energy gap (E_g) between HOMO and LUMO is 3.77 eV, which is comparable than that of [Pt(ppy)(ppyH)(Me)] ($E_g = 3.80$ eV).

6. Database survey

A survey of SciFinder (2021) for transition-metal complexes bearing the 2',6'-difluoro-2,3'-bipyridine moiety as a ligand gave 25 hits. They include reports on the crystal structures and photophysical properties of Ir^{III} and Pt^{II} complexes based on this ligand (CSD refcode HOVHAC, Lee *et al.*, 2009; OHUMUB01, Lee *et al.*, 2015; JUDZAL, Park *et al.*, 2015). The survey revealed no exact matches for the reported structure of the title complex. To the best of our knowledge, this is the first crystal structure reported for a platinum complex with the title ligand.

7. Synthesis and crystallization

All experiments were performed under a dry N_2 atmosphere using standard Schlenk techniques. All solvents were freshly distilled over appropriate drying reagents prior to use. All starting materials were purchased commercially and used

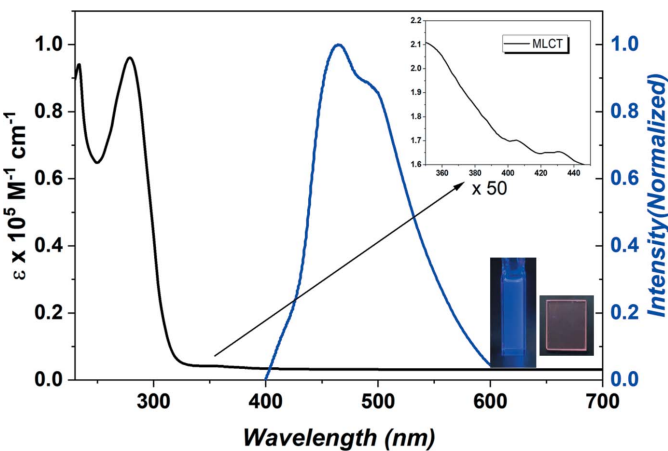


Figure 3

Absorption and emission of title compound at ambient temperature. Inset: extended absorption in the region of 350–450 nm.

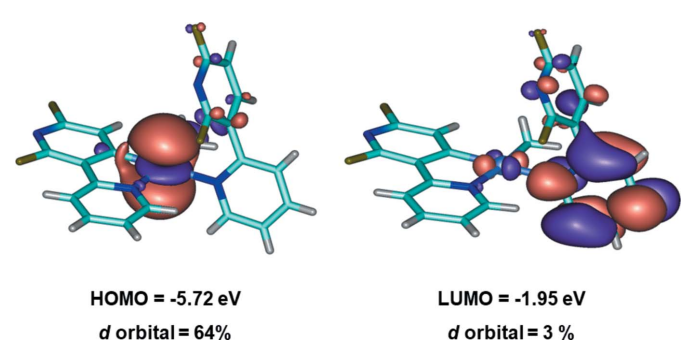


Figure 4

Isodensity surfaces and energy levels of the MOs mainly involved in the $S_0 \rightarrow S_1$ and $S_0 \rightarrow T_1$ transitions. (Isocontour value = 0.03.)

Table 3
Experimental details.

Crystal data	
Chemical formula	[Pt(CH ₃)(C ₁₀ H ₅ F ₂ N ₂)(C ₁₀ H ₆ F ₂ N ₂)]
<i>M</i> _r	593.45
Crystal system, space group	Monoclinic, <i>P</i> 2 ₁ / <i>c</i>
Temperature (K)	173
<i>a</i> , <i>b</i> , <i>c</i> (Å)	11.1590 (4), 11.4767 (4), 16.1918 (5)
β (°)	109.1050 (12)
<i>V</i> (Å ³)	1959.44 (12)
<i>Z</i>	4
Radiation type	Mo <i>K</i> α
μ (mm ⁻¹)	7.21
Crystal size (mm)	0.51 × 0.31 × 0.20
Data collection	
Diffractometer	Bruker APEXII CCD
Absorption correction	Multi-scan (<i>SADABS</i> ; Bruker, 2014)
<i>T</i> _{min} , <i>T</i> _{max}	0.258, 0.746
No. of measured, independent and observed [<i>I</i> > 2σ(<i>I</i>)] reflections	35428, 4873, 4088
<i>R</i> _{int}	0.050
(sin θ/λ) _{max} (Å ⁻¹)	0.667
Refinement	
<i>R</i> [F ² > 2σ(F ²)], <i>wR</i> (F ²), <i>S</i>	0.026, 0.066, 1.06
No. of reflections	4873
No. of parameters	271
H-atom treatment	H-atom parameters constrained
Δρ _{max} , Δρ _{min} (e Å ⁻³)	1.91, -1.66

Computer programs: *APEX2* and *SAINT* (Bruker, 2014), *SHELXS97* and *SHELXTL* (Sheldrick, 2008), *SHELXL2014/7* (Sheldrick, 2015), *DIAMOND* (Brandenburg, 2010) and *publCIF* (Westrip, 2010).

without further purification. The ¹H NMR spectrum was recorded on a JEOL 400 MHz spectrometer. The starting material, 2',6'-difluoro-2,3'-bipyridine was synthesized by a slight modification of the previous synthetic methodology reported by our group. (Kim *et al.*, 2018; Oh *et al.*, 2013). The title complex was also synthesized according to a previous report (Kang *et al.*, 2022b). Slow evaporation from a dichloromethane/hexane solution afforded yellow crystals suitable for X-ray crystallography analysis. Yield 75%. ¹H NMR (400 MHz, CD₂Cl₂): δ 8.97 (dd, *J* = 5.6, 2.0 Hz, 1H), 8.58 (dd, *J* = 8.0, 1.6 Hz, 1H), 8.05 (m, 2H), 7.88 (t, *J* = 8.0 Hz, 1H), 7.74 (m, 2H), 7.05 (m, 2H), 7.57 (td, *J* = 6.8, 1.2 Hz, 1H), 6.77 (dd, *J* = 8.0, 2.4 Hz, 1H), 0.72 (s, J_{Hpt} = 83.6 Hz, 3H). Analysis calculated for C₁₅H₁₄F₄N₄Pt; C 42.50; H 2.38; N 9.44; found: C 42.48, H 2.36, N 9.47%.

8. Refinement

Crystal data, data collection and crystal structure refinement details are summarized in Table 3. All H atoms were positioned geometrically and refined using a riding model, with C—H = 0.95 Å for Csp²—H, 0.98 Å for methyl C—H with *U*_{iso}(H) = 1.2–1.5*U*_{eq}(C).

Funding information

Funding for this research was provided by: National Research Foundation of Korea (grant No. 2022R1F1A1063758); Ministry of Trade, Industry and Energy, Korea Evaluation Institute of Industrial Technology (grant No. 20018956).

References

- Brandenburg, K. (2010). *DIAMOND*. Crystal Impact GbR, Bonn, Germany.
- Bruker (2014). *APEX2*, *SAINT* and *SADABS*. Bruker AXS Inc., Madison, Wisconsin, USA.
- Frisch, M. J., Trucks, G. W., Schlegel, H. B., Scuseria, G. E., Robb, M. A., Cheeseman, J. R., Montgomery, J. A. Jr., Vreven, T., Kudin, K. N., Burant, J. C., Millam, J. M., Iyengar, S. S., Tomasi, J., Barone, V., Mennucci, B., Cossi, M., Scalmani, G., Rega, N., Petersson, G. A., Nakatsuji, H., Hada, M., Ehara, M., Toyota, K., Fukuda, R., Hasegawa, J., Ishida, M., Nakajima, T., Honda, Y., Kitao, O., Nakai, H., Klene, M., Li, X., Knox, J. E., Hratchian, H. P., Cross, J. B., Bakken, V., Adamo, C., Jaramillo, J., Gomperts, R., Stratmann, R. E., Yazyev, O., Austin, A. J., Cammi, R., Pomelli, C., Ochterski, J. W., Ayala, P. Y., Morokuma, K., Voth, G. A., Salvador, P., Dannenberg, J. J., Zakrzewski, V. G., Dapprich, S., Daniels, A. D., Strain, M. C., Farkas, O., Malick, D. K., Rabuck, A. D., Raghavachari, K., Foresman, J. B., Ortiz, J. V., Cui, Q., Baboul, A. G., Clifford, S., Ciosowski, J., Stefanov, B. B., Liu, G., Liashenko, A., Piskorz, P., Komaromi, I., Martin, R. L., Fox, D. J., Keith, T., Al-Laham, M. A., Peng, C. Y., Nanayakkara, A., Challacombe, M., Gill, P. M. W., Johnson, B., Chen, W., Wong, M. W., Gonzalez, C. & Pople, J. A. (2004). *Gaussian 03*, Revision C.02. Gaussian, Inc., Wallingford CT, USA.
- Juliá, F., Bautista, D. & González-Herrero, P. (2016). *Chem. Commun.* **52**, 1657–1660.
- Juliá, F. & González-Herrero, P. (2016). *J. Am. Chem. Soc.* **138**, 5276–5282.
- Kang, J., Kim, S. C., Lee, J. Y. & Kang, Y. (2022a). *Dyes & Pigm.* **207**, 110770.
- Kang, J., Moon, S.-H., Paek, S. & Kang, Y. (2022b). *Can. J. Chem.* In the press. <https://doi.org/10.1139/cjc-2022-0093>.
- Kang, J., Zaen, R., Lee, J. H., Hwang, H., Park, K.-M., Kim, S. C., Lee, J. Y. & Kang, Y. (2022c). *Chem. Eng. J.* **431**, 134249.
- Kang, J., Zaen, R., Park, K.-M., Lee, K. H., Lee, J. Y. & Kang, Y. (2021). *Adv. Opt. Mater.* **9**, 2101233.
- Kim, M., Kim, J., Park, K.-M. & Kang, Y. (2018). *Bull. Korean Chem. Soc.* **39**, 703–706.
- Lee, C., Zaen, R., Park, K.-M., Lee, K. H., Lee, J. Y. & Kang, Y. (2018). *Organometallics*, **37**, 4639–4647.
- Lee, J., Park, H., Park, K. M., Kim, J., Lee, J. Y. & Kang, Y. (2015). *Dyes Pigments*, **123**, 235–241.
- Lee, S. J., Park, K. M., Yang, K. & Kang, Y. (2009). *Inorg. Chem.* **48**, 1030–1037.
- Oh, H., Park, K.-M., Hwang, H., Oh, S., Lee, J. H., Lu, J.-S., Wang, S. & Kang, Y. (2013). *Organometallics*, **32**, 6427–6436.
- Park, K.-M., Lee, J. & Kang, Y. (2015). *Acta Cryst. E71*, 354–356.
- SciFinder (2021). Chemical Abstracts Service: Columbus, OH, 2010; RN 58-08-2 (accessed October 7, 2022).
- Sheldrick, G. M. (2008). *Acta Cryst. A64*, 112–122.
- Sheldrick, G. M. (2015). *Acta Cryst. C71*, 3–8.
- Zaen, R., Park, K.-M., Lee, K. H., Lee, J. Y. & Kang, Y. (2019). *Adv. Opt. Mater.* **7**, 1901387.
- Zhang, H., Luo, Y., Yan, X., Cai, W., Zhao, A., Meng, Q. & Shen, W. (2020). *Inorg. Chim. Acta*, **501**, 119269.
- Westrip, S. P. (2010). *J. Appl. Cryst.* **43**, 920–925.

supporting information

Acta Cryst. (2022). E78, 1169-1172 [https://doi.org/10.1107/S2056989022010519]

Synthesis, crystal structure and DFT calculations of (2',6'-difluoro-2,3'-bipyridine- κN^2)[2,6-difluoro-3-(pyridin-2-yl)phenyl- $\kappa^2 C^1,N^3$]methylplatinum(II)

Suk-Hee Moon, Seohyeon Choi and Youngjin Kang

Computing details

Data collection: *APEX2* (Bruker, 2014); cell refinement: *SAINT* (Bruker, 2014); data reduction: *SAINT* (Bruker, 2014); program(s) used to solve structure: *SHELXS97* (Sheldrick, 2008); program(s) used to refine structure: *SHELXL2014/7* (Sheldrick, 2015); molecular graphics: *DIAMOND* (Brandenburg, 2010); software used to prepare material for publication: *SHELXTL* (Sheldrick, 2008) and *publCIF* (Westrip, 2010).

(2',6'-Difluoro-2,3'-bipyridine- κN^2)[2,6-difluoro-3-(pyridin-2-yl)phenyl- $\kappa^2 C^1,N^3$]methylplatinum(II)

Crystal data

[Pt(CH ₃)(C ₁₀ H ₅ F ₂ N ₂)(C ₁₀ H ₆ F ₂ N ₂)]	<i>F</i> (000) = 1128
<i>M_r</i> = 593.45	<i>D_x</i> = 2.012 Mg m ⁻³
Monoclinic, <i>P2₁/c</i>	Mo <i>Kα</i> radiation, λ = 0.71073 Å
<i>a</i> = 11.1590 (4) Å	Cell parameters from 9651 reflections
<i>b</i> = 11.4767 (4) Å	θ = 2.6–28.3°
<i>c</i> = 16.1918 (5) Å	μ = 7.21 mm ⁻¹
β = 109.1050 (12)°	<i>T</i> = 173 K
<i>V</i> = 1959.44 (12) Å ³	Block, yellow
<i>Z</i> = 4	0.51 × 0.31 × 0.20 mm

Data collection

Bruker APEXII CCD	4873 independent reflections
diffractometer	4088 reflections with $I > 2\sigma(I)$
φ and ω scans	R_{int} = 0.050
Absorption correction: multi-scan	$\theta_{\text{max}} = 28.3^\circ$, $\theta_{\text{min}} = 1.9^\circ$
(SADABS; Bruker, 2014)	$h = -14 \rightarrow 13$
$T_{\text{min}} = 0.258$, $T_{\text{max}} = 0.746$	$k = -15 \rightarrow 14$
35428 measured reflections	$l = -21 \rightarrow 21$

Refinement

Refinement on F^2	Hydrogen site location: inferred from
Least-squares matrix: full	neighbouring sites
$R[F^2 > 2\sigma(F^2)]$ = 0.026	H-atom parameters constrained
$wR(F^2)$ = 0.066	$w = 1/[\sigma^2(F_o^2) + (0.0339P)^2 + 1.3145P]$
S = 1.06	where $P = (F_o^2 + 2F_c^2)/3$
4873 reflections	$(\Delta/\sigma)_{\text{max}} = 0.002$
271 parameters	$\Delta\rho_{\text{max}} = 1.91 \text{ e \AA}^{-3}$
0 restraints	$\Delta\rho_{\text{min}} = -1.66 \text{ e \AA}^{-3}$

Special details

Geometry. All esds (except the esd in the dihedral angle between two l.s. planes) are estimated using the full covariance matrix. The cell esds are taken into account individually in the estimation of esds in distances, angles and torsion angles; correlations between esds in cell parameters are only used when they are defined by crystal symmetry. An approximate (isotropic) treatment of cell esds is used for estimating esds involving l.s. planes.

Fractional atomic coordinates and isotropic or equivalent isotropic displacement parameters (\AA^2)

	<i>x</i>	<i>y</i>	<i>z</i>	$U_{\text{iso}}^*/U_{\text{eq}}$
Pt1	0.79889 (2)	0.62391 (2)	0.38446 (2)	0.02333 (6)
F1	0.8075 (3)	0.4105 (2)	0.68292 (16)	0.0611 (7)
F2	1.1104 (2)	0.6711 (2)	0.70353 (13)	0.0498 (6)
F3	0.4034 (2)	0.9425 (2)	0.43326 (16)	0.0567 (7)
F4	0.7227 (2)	0.9395 (2)	0.32471 (16)	0.0525 (6)
N1	0.9578 (3)	0.7325 (2)	0.42974 (17)	0.0273 (6)
N2	0.9587 (3)	0.5417 (3)	0.69091 (18)	0.0356 (7)
N3	0.7423 (3)	0.6787 (2)	0.25218 (17)	0.0259 (6)
N4	0.5636 (3)	0.9383 (3)	0.37943 (19)	0.0374 (7)
C1	0.8571 (3)	0.5774 (3)	0.5081 (2)	0.0254 (7)
C2	0.8049 (4)	0.4979 (3)	0.5511 (2)	0.0333 (8)
H2	0.7332	0.4526	0.5197	0.040*
C3	0.8589 (4)	0.4860 (3)	0.6398 (2)	0.0363 (8)
C4	1.0080 (4)	0.6150 (3)	0.6493 (2)	0.0319 (8)
C5	0.9668 (3)	0.6381 (3)	0.5607 (2)	0.0259 (7)
C6	1.0230 (3)	0.7225 (3)	0.5166 (2)	0.0274 (7)
C7	1.1322 (4)	0.7899 (4)	0.5540 (2)	0.0404 (9)
H7	1.1767	0.7851	0.6149	0.048*
C8	1.1747 (4)	0.8630 (4)	0.5023 (3)	0.0493 (11)
H8	1.2493	0.9079	0.5273	0.059*
C9	1.1092 (4)	0.8711 (3)	0.4146 (3)	0.0437 (10)
H9	1.1380	0.9207	0.3781	0.052*
C10	0.9997 (4)	0.8051 (3)	0.3804 (2)	0.0359 (8)
H10	0.9530	0.8117	0.3200	0.043*
C11	0.4600 (4)	0.7447 (3)	0.2797 (3)	0.0381 (9)
H11	0.4238	0.6785	0.2454	0.046*
C12	0.4010 (4)	0.7948 (4)	0.3344 (3)	0.0406 (9)
H12	0.3245	0.7640	0.3392	0.049*
C13	0.4575 (4)	0.8898 (4)	0.3807 (3)	0.0390 (9)
C14	0.6162 (4)	0.8884 (3)	0.3281 (3)	0.0356 (9)
C15	0.5722 (3)	0.7921 (3)	0.2758 (2)	0.0292 (7)
C16	0.6394 (3)	0.7474 (3)	0.2168 (2)	0.0284 (7)
C17	0.5998 (4)	0.7774 (3)	0.1295 (2)	0.0380 (9)
H17	0.5262	0.8241	0.1059	0.046*
C18	0.6668 (4)	0.7397 (3)	0.0763 (2)	0.0382 (9)
H18	0.6413	0.7617	0.0164	0.046*
C19	0.7699 (4)	0.6705 (3)	0.1114 (2)	0.0364 (8)
H19	0.8172	0.6424	0.0763	0.044*
C20	0.8051 (4)	0.6414 (3)	0.1992 (2)	0.0342 (8)

H20	0.8771	0.5928	0.2231	0.041*
C21	0.6504 (4)	0.5106 (3)	0.3531 (2)	0.0383 (9)
H21A	0.6027	0.5169	0.2906	0.057*
H21B	0.6824	0.4309	0.3665	0.057*
H21C	0.5947	0.5294	0.3871	0.057*

Atomic displacement parameters (\AA^2)

	U^{11}	U^{22}	U^{33}	U^{12}	U^{13}	U^{23}
Pt1	0.02173 (9)	0.02615 (9)	0.01832 (7)	-0.00107 (5)	0.00136 (5)	-0.00167 (4)
F1	0.086 (2)	0.0583 (15)	0.0389 (13)	-0.0253 (15)	0.0204 (13)	0.0103 (12)
F2	0.0438 (14)	0.0766 (16)	0.0194 (10)	-0.0193 (13)	-0.0028 (9)	-0.0036 (10)
F3	0.0405 (14)	0.0813 (19)	0.0549 (15)	0.0043 (13)	0.0243 (12)	-0.0113 (14)
F4	0.0407 (13)	0.0626 (16)	0.0616 (15)	-0.0250 (12)	0.0267 (12)	-0.0259 (13)
N1	0.0235 (14)	0.0344 (16)	0.0218 (13)	-0.0019 (12)	0.0044 (11)	-0.0006 (11)
N2	0.0425 (18)	0.0406 (18)	0.0239 (14)	0.0026 (15)	0.0110 (13)	0.0027 (12)
N3	0.0252 (14)	0.0243 (14)	0.0231 (13)	-0.0043 (12)	0.0008 (11)	-0.0029 (11)
N4	0.0296 (17)	0.048 (2)	0.0330 (16)	-0.0036 (15)	0.0080 (13)	-0.0094 (14)
C1	0.0286 (18)	0.0247 (17)	0.0218 (15)	0.0005 (14)	0.0066 (13)	-0.0037 (13)
C2	0.039 (2)	0.0299 (18)	0.0281 (17)	-0.0070 (16)	0.0071 (15)	-0.0012 (14)
C3	0.048 (2)	0.033 (2)	0.0296 (17)	-0.0009 (17)	0.0154 (16)	0.0039 (15)
C4	0.0282 (19)	0.042 (2)	0.0219 (16)	0.0013 (16)	0.0025 (14)	-0.0040 (14)
C5	0.0211 (16)	0.0328 (19)	0.0223 (15)	0.0010 (14)	0.0051 (13)	-0.0029 (13)
C6	0.0244 (17)	0.0363 (19)	0.0205 (15)	-0.0004 (15)	0.0062 (13)	-0.0027 (13)
C7	0.037 (2)	0.058 (3)	0.0226 (16)	-0.0141 (19)	0.0048 (15)	-0.0071 (16)
C8	0.042 (2)	0.065 (3)	0.038 (2)	-0.029 (2)	0.0086 (18)	-0.0128 (19)
C9	0.044 (3)	0.054 (3)	0.034 (2)	-0.016 (2)	0.0139 (18)	-0.0024 (17)
C10	0.035 (2)	0.045 (2)	0.0272 (17)	-0.0077 (17)	0.0085 (15)	0.0037 (15)
C11	0.029 (2)	0.033 (2)	0.046 (2)	-0.0004 (16)	0.0039 (16)	0.0021 (16)
C12	0.0227 (19)	0.044 (2)	0.053 (2)	-0.0001 (17)	0.0097 (17)	0.0070 (19)
C13	0.028 (2)	0.055 (3)	0.034 (2)	0.0036 (18)	0.0094 (16)	0.0003 (17)
C14	0.032 (2)	0.040 (2)	0.0322 (19)	-0.0058 (16)	0.0069 (16)	-0.0042 (15)
C15	0.0227 (17)	0.0321 (19)	0.0266 (16)	0.0024 (15)	-0.0004 (13)	0.0061 (14)
C16	0.0265 (17)	0.0286 (18)	0.0241 (15)	-0.0045 (14)	0.0002 (13)	-0.0017 (13)
C17	0.037 (2)	0.041 (2)	0.0276 (17)	0.0062 (17)	-0.0014 (15)	0.0065 (15)
C18	0.049 (2)	0.037 (2)	0.0223 (16)	-0.0066 (18)	0.0031 (16)	0.0015 (14)
C19	0.046 (2)	0.036 (2)	0.0278 (17)	-0.0094 (18)	0.0136 (16)	-0.0063 (15)
C20	0.037 (2)	0.034 (2)	0.0293 (18)	0.0016 (16)	0.0073 (16)	-0.0023 (14)
C21	0.033 (2)	0.040 (2)	0.0319 (18)	-0.0073 (17)	-0.0022 (15)	-0.0036 (16)

Geometric parameters (\AA , $^\circ$)

Pt1—C1	1.966 (3)	C7—H7	0.9500
Pt1—C21	2.036 (4)	C8—C9	1.371 (6)
Pt1—N1	2.094 (3)	C8—H8	0.9500
Pt1—N3	2.120 (3)	C9—C10	1.389 (6)
F1—C3	1.352 (4)	C9—H9	0.9500
F2—C4	1.354 (4)	C10—H10	0.9500

F3—C13	1.339 (4)	C11—C15	1.386 (5)
F4—C14	1.342 (4)	C11—C12	1.390 (5)
N1—C10	1.340 (4)	C11—H11	0.9500
N1—C6	1.360 (4)	C12—C13	1.356 (6)
N2—C4	1.306 (5)	C12—H12	0.9500
N2—C3	1.316 (5)	C14—C15	1.382 (5)
N3—C20	1.343 (5)	C15—C16	1.484 (5)
N3—C16	1.356 (4)	C16—C17	1.379 (5)
N4—C14	1.297 (5)	C17—C18	1.383 (5)
N4—C13	1.314 (5)	C17—H17	0.9500
C1—C2	1.386 (5)	C18—C19	1.361 (6)
C1—C5	1.423 (5)	C18—H18	0.9500
C2—C3	1.371 (5)	C19—C20	1.386 (5)
C2—H2	0.9500	C19—H19	0.9500
C4—C5	1.382 (5)	C20—H20	0.9500
C5—C6	1.461 (5)	C21—H21A	0.9800
C6—C7	1.402 (5)	C21—H21B	0.9800
C7—C8	1.374 (6)	C21—H21C	0.9800
C1—Pt1—C21	92.94 (14)	C10—C9—H9	120.8
C1—Pt1—N1	81.10 (12)	N1—C10—C9	122.3 (3)
C21—Pt1—N1	174.00 (12)	N1—C10—H10	118.8
C1—Pt1—N3	177.73 (12)	C9—C10—H10	118.8
C21—Pt1—N3	89.33 (13)	C15—C11—C12	119.4 (4)
N1—Pt1—N3	96.63 (10)	C15—C11—H11	120.3
C10—N1—C6	119.7 (3)	C12—C11—H11	120.3
C10—N1—Pt1	125.6 (2)	C13—C12—C11	116.9 (4)
C6—N1—Pt1	114.7 (2)	C13—C12—H12	121.5
C4—N2—C3	113.7 (3)	C11—C12—H12	121.5
C20—N3—C16	117.6 (3)	N4—C13—F3	114.5 (3)
C20—N3—Pt1	120.3 (2)	N4—C13—C12	126.2 (4)
C16—N3—Pt1	122.0 (2)	F3—C13—C12	119.3 (4)
C14—N4—C13	114.9 (3)	N4—C14—F4	115.2 (3)
C2—C1—C5	116.3 (3)	N4—C14—C15	127.0 (4)
C2—C1—Pt1	129.6 (3)	F4—C14—C15	117.7 (3)
C5—C1—Pt1	114.1 (2)	C14—C15—C11	115.5 (3)
C3—C2—C1	118.6 (3)	C14—C15—C16	121.2 (3)
C3—C2—H2	120.7	C11—C15—C16	123.2 (3)
C1—C2—H2	120.7	N3—C16—C17	121.4 (3)
N2—C3—F1	113.7 (3)	N3—C16—C15	117.7 (3)
N2—C3—C2	127.0 (3)	C17—C16—C15	120.9 (3)
F1—C3—C2	119.3 (3)	C16—C17—C18	120.3 (4)
N2—C4—F2	112.4 (3)	C16—C17—H17	119.9
N2—C4—C5	127.3 (3)	C18—C17—H17	119.9
F2—C4—C5	120.4 (3)	C19—C18—C17	118.5 (3)
C4—C5—C1	117.1 (3)	C19—C18—H18	120.7
C4—C5—C6	125.7 (3)	C17—C18—H18	120.7
C1—C5—C6	117.1 (3)	C18—C19—C20	119.1 (4)

N1—C6—C7	119.7 (3)	C18—C19—H19	120.4
N1—C6—C5	113.0 (3)	C20—C19—H19	120.4
C7—C6—C5	127.4 (3)	N3—C20—C19	123.1 (4)
C8—C7—C6	119.9 (3)	N3—C20—H20	118.5
C8—C7—H7	120.0	C19—C20—H20	118.5
C6—C7—H7	120.0	Pt1—C21—H21A	109.5
C9—C8—C7	119.9 (4)	Pt1—C21—H21B	109.5
C9—C8—H8	120.1	H21A—C21—H21B	109.5
C7—C8—H8	120.1	Pt1—C21—H21C	109.5
C8—C9—C10	118.5 (4)	H21A—C21—H21C	109.5
C8—C9—H9	120.8	H21B—C21—H21C	109.5
C5—C1—C2—C3	2.0 (5)	C8—C9—C10—N1	-1.4 (6)
Pt1—C1—C2—C3	-175.8 (3)	C15—C11—C12—C13	0.7 (6)
C4—N2—C3—F1	-179.7 (3)	C14—N4—C13—F3	-179.5 (3)
C4—N2—C3—C2	-0.2 (6)	C14—N4—C13—C12	0.2 (6)
C1—C2—C3—N2	-0.9 (6)	C11—C12—C13—N4	-0.7 (6)
C1—C2—C3—F1	178.6 (3)	C11—C12—C13—F3	178.9 (4)
C3—N2—C4—F2	180.0 (3)	C13—N4—C14—F4	178.2 (3)
C3—N2—C4—C5	0.0 (6)	C13—N4—C14—C15	0.4 (6)
N2—C4—C5—C1	1.2 (6)	N4—C14—C15—C11	-0.4 (6)
F2—C4—C5—C1	-178.8 (3)	F4—C14—C15—C11	-178.1 (3)
N2—C4—C5—C6	178.7 (3)	N4—C14—C15—C16	177.0 (4)
F2—C4—C5—C6	-1.2 (5)	F4—C14—C15—C16	-0.8 (5)
C2—C1—C5—C4	-2.1 (5)	C12—C11—C15—C14	-0.2 (5)
Pt1—C1—C5—C4	176.0 (2)	C12—C11—C15—C16	-177.5 (3)
C2—C1—C5—C6	-179.9 (3)	C20—N3—C16—C17	0.5 (5)
Pt1—C1—C5—C6	-1.8 (4)	Pt1—N3—C16—C17	-176.6 (3)
C10—N1—C6—C7	1.2 (5)	C20—N3—C16—C15	-178.0 (3)
Pt1—N1—C6—C7	179.1 (3)	Pt1—N3—C16—C15	5.0 (4)
C10—N1—C6—C5	-178.7 (3)	C14—C15—C16—N3	81.1 (4)
Pt1—N1—C6—C5	-0.7 (4)	C11—C15—C16—N3	-101.7 (4)
C4—C5—C6—N1	-175.9 (3)	C14—C15—C16—C17	-97.3 (4)
C1—C5—C6—N1	1.6 (4)	C11—C15—C16—C17	79.8 (5)
C4—C5—C6—C7	4.2 (6)	N3—C16—C17—C18	-1.5 (5)
C1—C5—C6—C7	-178.2 (4)	C15—C16—C17—C18	176.9 (3)
N1—C6—C7—C8	-1.9 (6)	C16—C17—C18—C19	1.6 (6)
C5—C6—C7—C8	178.0 (4)	C17—C18—C19—C20	-0.8 (6)
C6—C7—C8—C9	0.9 (7)	C16—N3—C20—C19	0.4 (5)
C7—C8—C9—C10	0.7 (7)	Pt1—N3—C20—C19	177.5 (3)
C6—N1—C10—C9	0.5 (6)	C18—C19—C20—N3	-0.2 (6)
Pt1—N1—C10—C9	-177.3 (3)		

Hydrogen-bond geometry (\AA , $^\circ$)

$D\cdots H$	$D—H$	$H\cdots A$	$D\cdots A$	$D—H\cdots A$
C7—H7 \cdots F2	0.95	2.24	2.858 (4)	122

C12—H12···F1 ⁱ	0.95	2.44	3.259 (5)	144
C20—H20···N2 ⁱⁱ	0.95	2.45	3.385 (5)	167

Symmetry codes: (i) $-x+1, -y+1, -z+1$; (ii) $-x+2, -y+1, -z+1$.